

# Computational Determination of Reactivity Descriptors, Vibrational Analysis and Nuclear Magnetic Resonance of (E)-5-oxo-1-phenyl-4-(2-phenylhydrazono)-4,5-dihydro-1H-pyrazole-3-carbaldehyde

Nagwa M. M. Hamada<sup>a\*</sup>, Mohamed A. El Sekily<sup>b</sup>, Sohila H. Mancy<sup>c</sup>

<sup>a,c</sup>Department of Physics and Chemistry, Faculty of Education, University of Alexandria, 21526 Alexandria, Egypt

<sup>b</sup>Department of Chemistry, Faculty of Science, University of Alexandria, 21321 Alexandria, Egypt

<sup>a</sup>Email: [sohaylamansy@gmail.com](mailto:sohaylamansy@gmail.com)

<sup>b</sup>Email: [prof\\_dr\\_m\\_a\\_elsekily@yahoo.com](mailto:prof_dr_m_a_elsekily@yahoo.com)

## Abstract

The title compound, pyrazole carbaldehyde have been optimized using Gaussian 9 software program, via density functional theory framework (DFT/B3LYP) by 6-311G (d, p) basis set, the output file was visualize using Gaussian view program, geometric properties, thermochemical and reactivity descriptors such as ionization potential (IP), electron affinity (EA), electronegativity ( $\chi$ ), chemical potential ( $\mu$ ), hardness ( $\eta$ ), softness ( $\sigma$ ), electrophilicity index ( $\omega$ ) and nucleophilicity index (N) were calculated. Mapping of electrostatic surface potential (MESP) allow us to establish trends that enable making predictions about the reactive sites of the studied compound. Besides, the optimized structure is subjected to frequency analysis at the same level of theory to obtain thermodynamic correction values. Vibrational assignments and nuclear magnetic resonance (<sup>1</sup>H- & <sup>13</sup>C-NMR) chemical shifts of the molecule were calculated by gauge independent atomic orbital (GIAO) method using the CPCM model, and mapping of current density shielding of proton and carbon nucleus of the aldehyde group shied light on the molecular properties and reactivity of 5-oxo-1-phenyl-4-(2-phenylhydrazono)-4,5-dihydro-1H-pyrazole-3-carbaldehyde .

**Keywords:** Pyrazole carbaldehyde; DFT; Chemical potential; Hardness; Shielding density.

---

\* Corresponding author

## 1. Introduction

At the end of the 1980s of the twentieth century, ab initio Hartree-Fock (HF) calculations [1], enabled the study of the molecular mechanism of many organic reactions by characterizing the stationary points involved in a reaction. The electron density is more attractive and effective in explaining properties where it is measurable depends only on the Cartesian axes, x, y, and z. The fact that the ground state properties are functionals of the electron density  $\rho(\mathbf{r})$  was introduced by Hohenberg and Kohn [2] and it is the basic framework for modern Density functional (DF) methods [3], where the total ground state energy of an electron system can be written as a functional of the electronic density. At the end of the 20th century, a new theory based on the studying of the electronic structure of the matter was developed, known as Density Functional Theory (DFT), after its applications [4-7] a few decades ago, DFT has been recognized as a powerful tool to provide theoretical insights into chemical reactivity and how this influences the synthesis of different heterocyclic compounds, [8-15]. The split-valence basis sets were introduced by John Pople and his group in the late 1970s. There are an expansion of basis sets to make the total function more accurate and reliable. In general, polarization functions significantly improve the description of molecular geometries (bond lengths and angles) as well as molecular relative energies. The use of the density functional theory (DFT) calculations for predicting the molecular structure, as well as spectroscopic properties of organic compounds, are of great interest, and the selection of the proper basis set for the optimization of the studied molecule is very important. [16-19]. It has been reported that a large number of interesting pharmaceutical heterocyclic derivatives have been synthesized using the title compound 5-oxo-1-phenyl-4-(2-phenylhydrazono)-4,5-dihydro-1H-pyrazol-3-yl)-3-carbaldehyde, this attract our attention to study theoretically the activity of the pyrazole-aldehyde as a reaction intermediate in organic synthesis [20-22]. From this point of view, DFT calculations have been applied on the title aldehyde computed at The Lee, Yang, and Parr Correlation Energy Functional DFT/B3LYP at the triply split valence basis set 6311G (d,p) to generate quantum mechanical descriptors used in quantitative structure-activity relationship (QSAR) to explain its geometrical and energetic properties. Experimentally obtained physical and spectroscopic properties will be presented and validated by theoretical parameters related to the molecular reactivities such as electronegativity, dipole moment, electrophilicity, chemical potential, softness and hardness which are obtained by quantum chemical computations using DFT approximations [14,15, 23-27]. The electrostatic surface potential maps (ESP) maps of the energetically optimized molecules will also be reported [28,29].

## 2. Materials and Methods

Computations were performed using, ab initio/ DFT /B3LYP [30,31] from Gaussian 09 program package, GaussView 05 program [32-34]. was used to get the graphical presentations of calculated IR and  $^1\text{H-NMR}$  spectra. Harmonic vibrational frequencies of the optimized geometries were calculated by employing the widely used B3LYP /6-311G (d,p) model, in order to verify that they are true minima (with zero imaginary frequencies). The calculation of  $^1\text{H NMR}$  chemical shifts was performed by Gauge Induced atomic orbital (GIAO) method at the same level of theory.

## 3. Results and Discussion

### 3.1. Optimization calculations

The aim of the present work was to describe and characterize the molecular structure, vibrational frequencies and chemical shifts of the starting pyrazole carbaldehyde. The title compound was computed using DFT/B3LYP 6311 G (d,p) in gas phase and in acetonitrile as aprotic solvent, the results showed that there is no significant difference between the data obtained from both media, and this reflects that there is no solvent effect by acetonitrile, so we herein discuss the results obtained from the study in the gas phase only. The optimized structure with Mulliken charge numbers of the computed compound is shown in **Figure 1**.

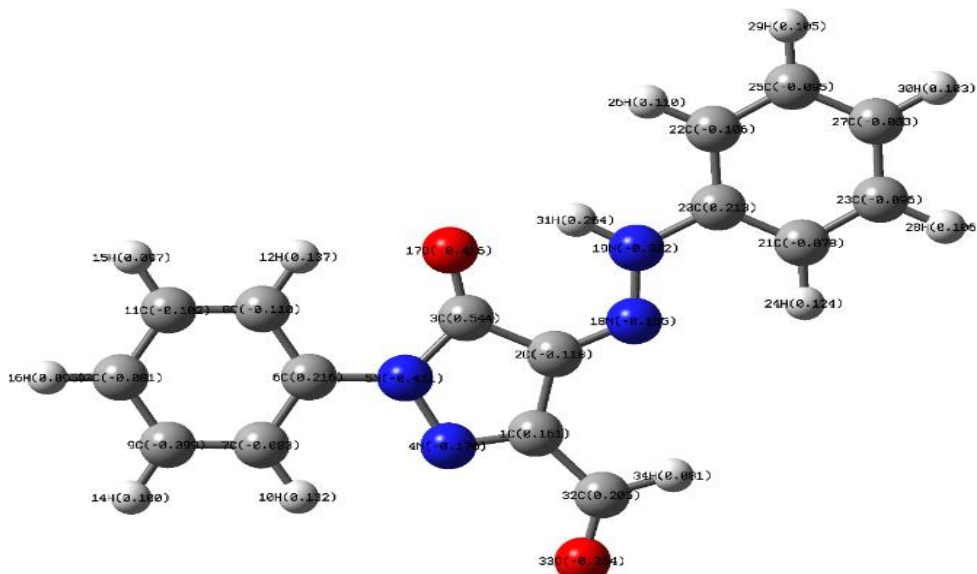


**Figure 1:** Optimized structure of the title compound calculated

The plots display the total energy of the optimized structure is shown in **Figure 2**.

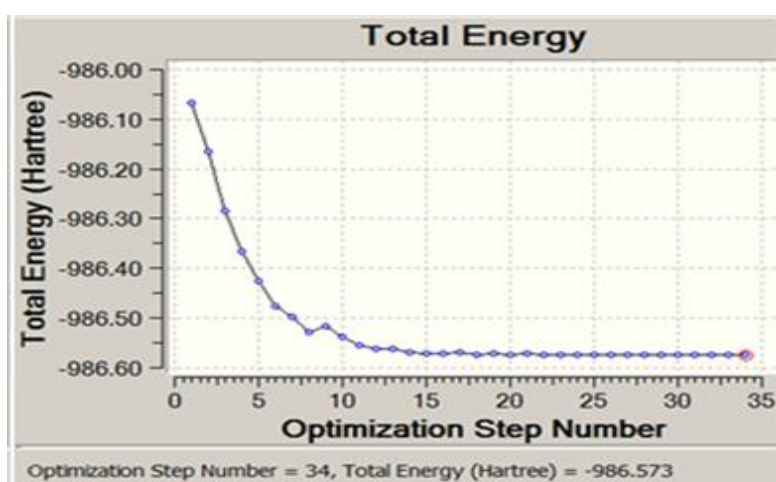


**Figure 2:** Total energy optimization of the title compound

3.2. Mulliken Charges and Geometrical Parameters

The Mulliken atomic charges of the studied compound are shown in **Table 1**. The charges at all the carbon atoms have negative values except that at C-3 (0.295150), C-20 (0.213292), C-32 (0.205287), C-2 (0.136294) and C-6 (0.086755), which can be responsible for nucleophilic attack centers. The large negatively charged atoms are O-17(-0.415732), N-19 (- 0.322440), N-5(-0.320278), O-33(-0.264034), N-18 (-0.155118), N-4(-0.152470). It is interesting to note the difference in distances of the two oxygen atoms of the carbonyl groups, the bond length of the carbonyl of the pyrazole ring (C3-O17) appeared to be 1.43 Å which is longer than that of the carbonyl of the aldehyde group (C32-O33) which appeared to be 1.2273 Å , There is one kind of intermolecular hydrogen bonding interaction, hydrogen bonding interactions between the oxygen atom of the pyrazole ring and the hydrogen 12 of the aromatic ring [3C=O17.....H12]; ( 1.4731 Å), bond lengths, and the average angles within the molecule are in a good agreement with those reported in the literature [35, 36]. Selected bond distances and related angles are collected in Table 1.

**Table 1:** Mulliken Charge, bond lengths (Å) and selected bond angles(°) of the title compound calculated at DFT/B3LYP/6-311G (d,p)

Mulliken Charges		Bond lengths (Å)		Bond angles (°)	
C-1	-0.026303	(C-1, C-2)	1.5219	(C-2,C-1,N-4)	107.954
C-2	0.136294	(C-1, N-4)	1.5222	(C-2,C-1,C-32)	110.507
C-3	0.295150	(C-1, C-32)	1.54	(N-4,C-1,C3-2)	110.534
N-4	-0.152470	(C-2, C-3)	1.5219	(C-1,C-2,C-3)	107.940
N-5	-0.320278	(C-2, N-18)	1.47	(C-1,C-2,N-18)	110.317
C-6	0.086755	(C-3, N-5)	1.522	(C-3,C-2,N-18)	110.332
C-7	-0.031808	(C-3, O-17)	1.43	(C-2,C-3,N-5)	107.914
C-8	-0.109997	(N-4, N-5)	1.522	(C-2,C-3,O-17)	110.333
C-9	-0.098779	(N-5, N-6)	1.47	(N-5,C-3,N-17)	110.327
H-10	0.132139	(C-6, C-7)	1.3952	(C-1,N-4,N-5)	107.974
C-11	-0.101914	(C-6, C-8)	1.3948	(C-3,N-5,N-4)	107.959
H-12	0.137239	(C-7, C-9)	1.3947	(C-3,N-5,C-6)	110.507
C-13	-0.081483	(C-7, H-10)	1.0997	(N-4,N-5,C-6)	110.547
H-14	0.099857	(C-8, C-11)	1.3951	(N-5,C-6,C-7)	119.997
H-15	0.097334	(C-8, H-12)	1.0996	(N-5,C-6,C-8)	120.004
H-16	0.095330	(C-9, C-13)	1.3954	(C-7,C-6,C-8)	119.999
O-17	-0.415732	(C-9, H-14)	1.0997	(C-6,C-7,C-9)	120.009
N-18	-0.155118	(C-11, C-13)	1.3948	(C-6,C-7,H-10)	119.981
N-19	-0.322440	(C-11, H-15)	1.0998	(C-9,C-7,H-10)	120.011
C-20	0.213292	(H-12, O-17)	1.4731	(C-6,C-8,C-11)	120.0
C-21	-0.077706	(C-13, H-16)	1.0997	(C-6,C-8,H-12)	120.008
C-22	-0.105951	(N-18, N-19)	1.232	(C-11,C-8, H-12)	119.992
C-23	-0.095728	(N-19, C-20)	1.47	(C-7, C-9, C-13)	119.994
H-24	0.123691	(N-19, H-31)	1.2566	(C-7, C-9, H-14)	120.013
C-25	-0.094613	(C-20, C-21)	1.3952	(C-13, C-9, H-14)	119.993
H-26	0.110329	(C-20, C-22)	1.3948	(C-8, C-11,C-13)	120.005
C-27	-0.083064	(C-21, C-23)	1.3947	(C-8,C-11,H-15)	119.984
H-28	0.105762	(C-21, H-24)	1.0997	(C13,C11,H15)	120.011
H-29	0.104745	(C-22 ,C-25)	1.3951	(C-9,C-13,C-11)	119.994
H-30	0.103329	(C-22, H-26)	1.0996	(C-9,C-13,H-16)	119.981
H-31	0.263615	(C-23, C-27)	1.3954	(C-11,C-13,H-16)	120.025
C-32	0.205287	(C-23, H-28)	1.0997	(N-18,N-19,H-31)	96.975
O-33	-0.264034	(C-25, C-27)	1.3948	(C-20,N-19,H-31)	83.025
H-34	0.081261	(C-25, H-29)	1.0998	(N-19,C-20,C-21)	119.997
		(C-27, H-30)	1.0997	(N-19,C-20,C-22)	120.004
		(C-32, O-33)	1.2273	(C-21,C-20,C-22)	119.999
		(C-32, H-34)	1.1105	(C-20,C-21,C-23)	120.009

### 3.3. *activity descriptors of the title compound.*

The quantum chemical descriptors of the title compound were calculated using DFT/B3LYP /6311 G (d,p) in gas phase, all the calculated descriptors [37-40] depends mainly on the energy of the frontier molecular orbitals  $E_{\text{HOMO}}$  (High occupied molecular orbital) and  $E_{\text{LUMO}}$  (Low unoccupied molecular orbital) , the ground state plot for the frontier molecular orbitals of the title compound is shown in **Figure 3**.

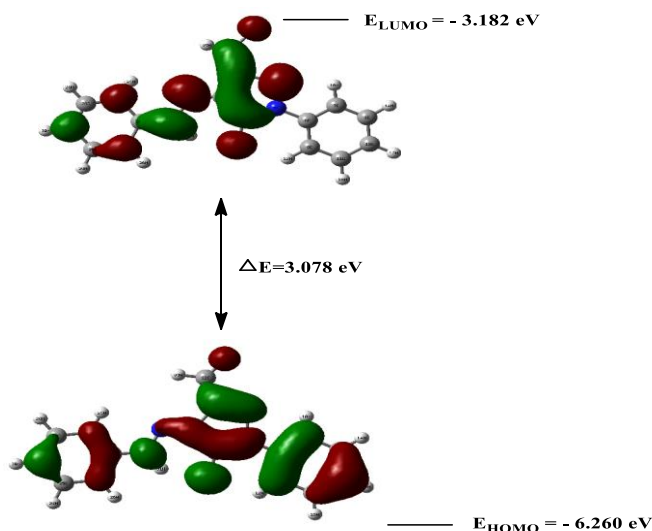


**Figure 3:** The ground state plots for the frontier molecular orbitals of the title compound .

In general chemical potential is the link between structure and reactivity as the greater chemical potential of studied compounds the greater its reactivity, the defined index of chemical potential ( $\mu$ ) is depends on the value of the electronegativity index ( $\chi$ ) which is the mean value of  $E_{\text{HOMO}}$  and  $E_{\text{LUMO}}$ , defined in terms of ionization energy (IP) and electron affinity (EA) as follows:  $\chi = (\text{IP} + \text{EA})/2$  and consequently the chemical potential ( $\mu$ ) =  $-\chi$ , the hardness is given by:  $\eta = 0.5 (E_{\text{LUMO}} - E_{\text{HOMO}})$ , softness ( $\sigma$ ) =  $1/\eta$ . As electrophilicity/nucleophilicity are useful concepts to explain electronic aspects of reactivity, selectivity, substituent effects, solvent effects, etc., the development of such scales becomes strongly justified. Within this point of view, the electrophilicity index ( $\omega = \mu^2/2\eta$ ) which measures the total ability to attract electrons, shows the tendency of an electrophile to acquire an extra amount of electron density, and the resistance of a molecule to exchange electron density with the environment given by the chemical hardness ( $\eta$ ) & softness ( $\sigma$ ) has shown to be a powerful tool. Furthermore, there are many attempts to define a nucleophilicity index, simple index was chosen for the nucleophilicity (N) which explain the maximum number of electrons that an electrophile can acquire, based on the HOMO energy, within DFT calculations, explain the reactivity of the organic material towards electrophiles [11,37,38]. The simple nucleophilicity index (N) is defined as  $N = E_{\text{HOMO}} (\text{eV}) + 9.12 (\text{eV})$ , where -9.12 is the energy of the HOMO of tetracyano ethylene (TCE), this nucleophilicity scale is referred to TCE and taken as a reference because TCE exhibits the lowest HOMO energy (= -9.12 eV). For instance, Roy and his colleagues [39] proposed the local hardness and softness based on DFT reactivity descriptors predict both intramolecular and intermolecular nucleophilic attacks on carbonyl compounds. On the other hand, Chattaraj and his colleagues suggested that the inverse of electrophilicity ( $x$ ) can also be a valid measure of nucleophilicity [40]. The

activation parameters of the starting pyrazol-carbaldehyde has been calculated according to the previous equations. From the results depicted in **Table 2** we can conclude that, the target molecule with high electrophilicity index ( $\omega$ )= 7.241eV and small value of nucleophilicity index = 2.86 is considered to be more likely attacked by a nucleophile, which is in agreement with the suggested mechanisms for the synthesized of heterocyclic compounds from the target compound in our recent article [22]. Also, the high value of the chemical potential (-4.721 eV) confirm our conclusion.

**Table 2:** Reactivity descriptors of the studied compound

Parameter	Value
Homo energy (eV)	-6.260
Lumo energy (eV)	-3.182
Energy gap (eV)	3.078
Ionization potential IP ( $-E_{\text{HOMO}}$ )	6.260
Electron affinity EA ( $-E_{\text{LUMO}}$ )	3.182
Electronegativity $\chi = (\text{IP} + \text{EA})/2$	4.721
Chemical potential $\mu = -\chi$	-4.721
Hardness $\eta = (\text{IP} - \text{EA})/2$	1.539
softness ( $\sigma$ )=1/ $\eta$	0.650
Electrophilicity index ( $\omega$ ) = $\mu^2/ 2\eta$	7.241
Nucleophilicity = $E_{\text{HOMO}} + 9.12$	2.86

### 3.4. Molecular electrostatic potential

Molecular electrostatic potential (MESP) diagram has been also used to predict the reactive sites for electrophilic and nucleophilic attack, as well as hydrogen bonding interaction [41-43], the MEP of the studied compound **1** calculated using B3LYP method with 6-311G (d,p) basis set is shown in **Figure 4**. This figure provides a visual representation of the chemically active sites and comparative reactivity of atoms. Potential increases in the order red < orange < yellow < green < blue. The map represents that the region of maximum negative electrostatic potential is situated around the aldehyde group with MEP value around -6.822 a.u and the most positive region is found at phenyl hydrazone moiety & with a value of +6.822 a.u.

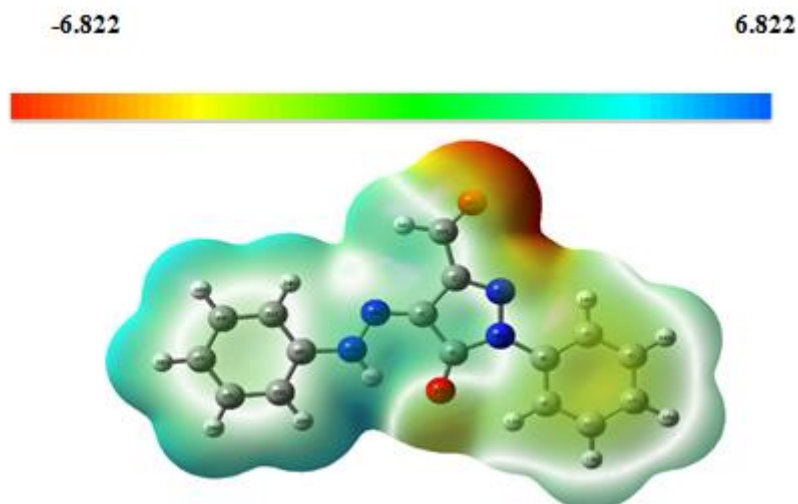


**Figure 4:** Electron density from total SCF density mapped with (ESP) of title compound (isovalue =0.0004).

### 3.5. Thermochemistry analysis

**Table 3:** Thermodynamic parameters of the title compound calculated using B3LYP/6-311G(d,p)

Parameters	B3LYP/6-311 G(d,p)
Rotational temperatures (Kelvin)	0.02741 0.00632 0.00513
Rotational constants (GHZ)	0.57121 0.13162 0.10697 X Y Z
Zero-point vibrational energy (Kcal/mol)	160.38587
Total Energy ( Hartree )	-986.573
Dipole moment	5.173
Electronic and zero-point Energies (Hartree )	-986.317637
Electronic and thermal Energies (Hartree )	-986.299956
Electronic and thermal Enthalpies (Hartree )	-986.299012

The computed vibration frequency of the pyrazole carbaldehyde, using DFT-B3LYP/6-311G (d,p) method , show some thermodynamic parameter values reflecting molecular polarities and the stability of the molecule.the target compound is asymmetric polar molecule, the computed total energy and thermodynamic parameters reflect the stability of the molecule. **Table 3** shows different thermodynamic parameters of target molecule and the dipole moment calculation value. Standard enthalpies of formation are evaluated using calculated energies, zero point vibration energy (ZPVE), plus thermal contributions (to 298K) the calculated total energy is corrected by the ZPVE.

### 3.6. Vibrational analysis

Computed harmonic frequencies of pyrazole carbaldehyde, shown in **Figure 5**. **Table 4** contains experimental and scaled calculated wave numbers, correlation between the experimental and

theoretical wave numbers at B3LYP/6311G basis set, showed a good linear correlation (**Figure 6**) with a regression coefficient of  $R^2 = 0.9979$ .

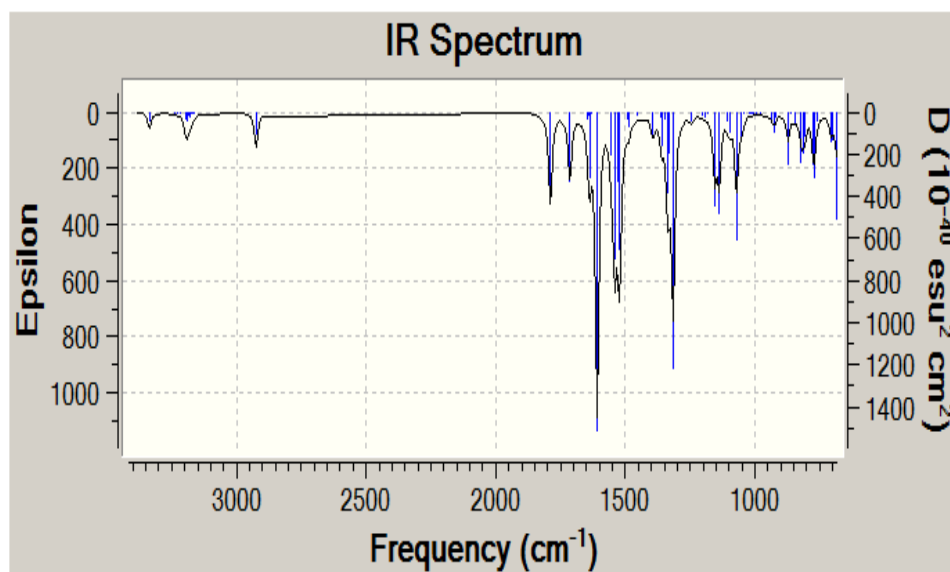


**Figure 5:** Computed harmonic frequencies of title compound.

**Table 4:** Experimental FT-IR and calculated vibrational frequencies in cm<sup>-1</sup> for the title compound

Experimental	Calculated	Vibrational assignment
3250	3335	-N <sub>19</sub> -H <sub>31</sub> stretching
3210	3217	Symmetric C-H stretching Aromatic
2825	2924	Symmetric C <sub>32</sub> -H <sub>34</sub>
1760	1789	Symmetric C <sub>32</sub> =O <sub>33</sub> stretching
1638	1713	Symmetric C <sub>3</sub> =O <sub>17</sub> stretching
1548	1553	C <sub>2</sub> =N <sub>18</sub> stretching
1536	1540	C <sub>1</sub> =N <sub>4</sub> stretching

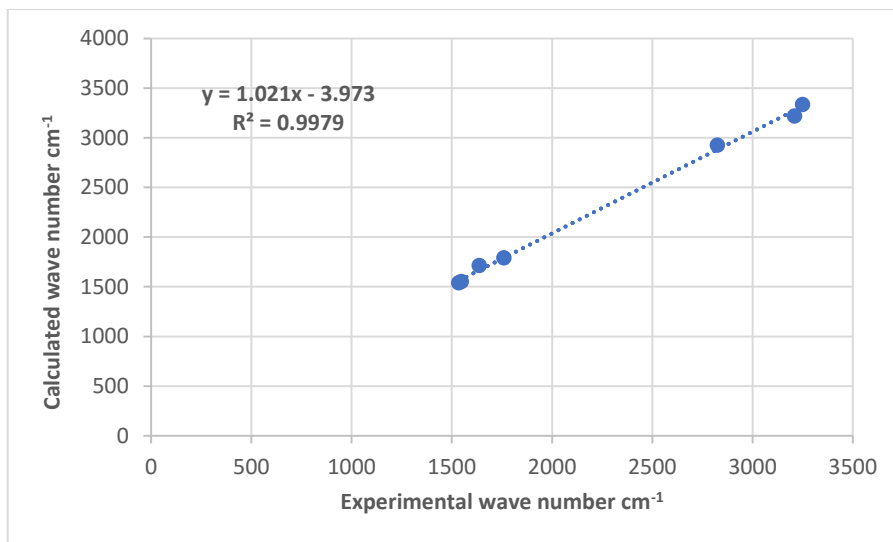


**Figure 6:** Correlation graph between experimental and calculated wave numbers.

### 3.7. Nuclear Magnetic Resonance studies

The optimized file of the studied compound was computed as NMR job at the same level of theory using The gauge-including atomic orbital (GIAO/ CPCM) method, and DMSO as solvent as shown in the screenshot of the out put wordPad file . **Figure 7**

```

-----
Polarizable Continuum Model (PCM)
=====
Model                : C-PCM.
Atomic radii         : UFF (Universal Force Field).
Polarization charges : Total charges.
Charge compensation  : None.
Solution method      : Matrix inversion.
Cavity type          : Scaled VdW (van der Waals Surface)
(Alpha=1.100).
Cavity algorithm     : GePol (No added spheres)
                    : Default sphere list used, NSphG= 34.
                    : Lebedev-Laikov grids with approx. 5.0

points / Ang**2.    Smoothing algorithm: Karplus/York (Gamma=
1.0000).
gaussians, with    Polarization charges: spherical
                    point-specific
exponents (IZeta= 3). Self-potential: point-specific (ISelfS=
7).
                    Self-field : sphere-specific E.n sum
rule (ISelfD= 2).   Solvent : DiMethylSulfoxide, Eps= 46.826000 Eps
(inf)= 2.007889
-----

```

**Figure 7:** Screenshot of the out put wordPad file

From the output file of the NMR job, the results showed that the calculated chemical shift for the studied compound (**Figure 8 & 9**) for both <sup>1</sup>H-NMR and <sup>13</sup>C-NMR were in good correlation with the experimental one (**Table 5**) with a regression coefficient of  $R^2 = 0.9785$  &  $0.9549$  for <sup>1</sup>H-NMR and <sup>13</sup>C-NMR respectively. (**Figure 10 & 11**).

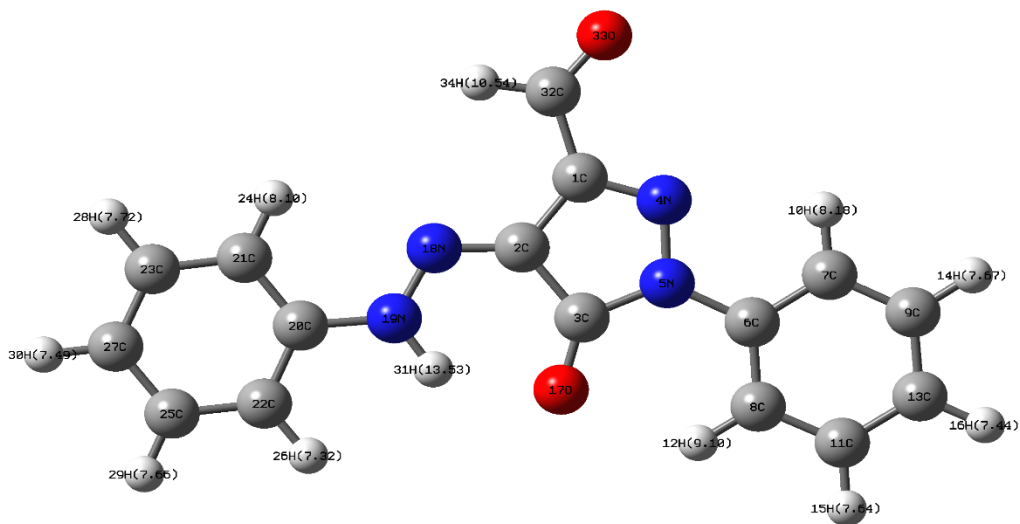


**Figure 8:** Optimized structure of the title compound with calculated <sup>1</sup>H-NMR chemical shift (ppm).

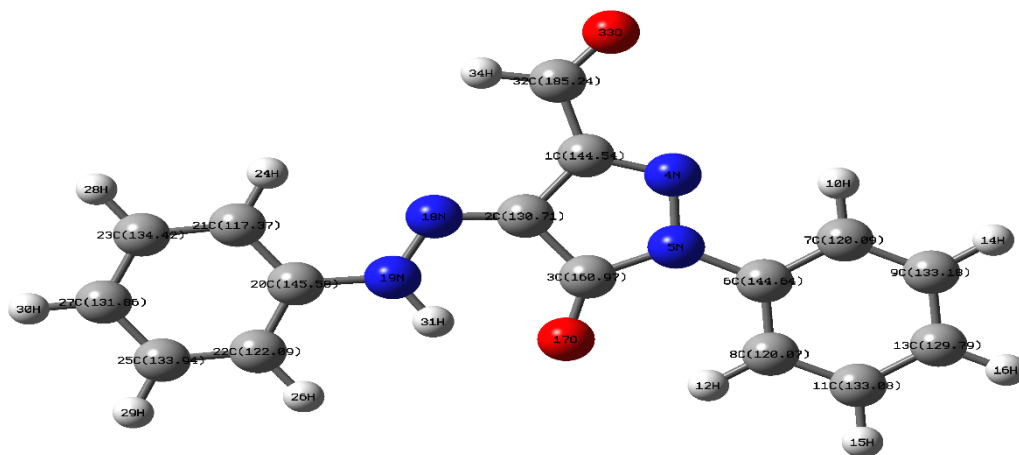


**Figure 9:** Optimized structure of the title compound with <sup>13</sup>C-NMR chemical shift (ppm).

**Table 5:** Experimental and calculated  $^{13}\text{C}$ -NMR &  $^1\text{H}$ -NMR chemical shift (ppm).

Carbon atom	Experimental $^{13}\text{C}$ -NMR chemical shift (ppm)	Calculated $^{13}\text{C}$ -NMR chemical shift (ppm)	Hydrogen atom	Experimental $^1\text{H}$ -NMR chemical shift(ppm)	Calculated $^1\text{H}$ -NMR chemical shift (ppm)
C-32	194.000	185.241	H-31	11.700	13.528
C-3	157.500	160.974	H-34	9.500	10.540
C-20	143.000	145.576	H-12	8.900	9.096
C-6	140.300	144.637	H-10	8.060	8.179
C-1	136.800	144.544	H-24	7.793	8.100
C-2	136.800	130.711	H-28	7.550	7.722
C-23	129.500	134.423	H-14	7.231	7.673
C-25	129.500	133.936	H-29	7.220	7.660
C-9	128.900	133.176	H-15	7.200	7.642
C-11	128.900	133.075	H-30	7.130	7.493
C-13	128.000	129.793	H-16	7.120	7.440
C-27	122.400	131.860	H-26	7.100	7.320
C-22	113.900	122.094	-	-	-
C-7	118.500		-	-	-
C-8	118.500	120.091	-	-	-
C-21	113.900	120.065	-	-	-
		117.371			

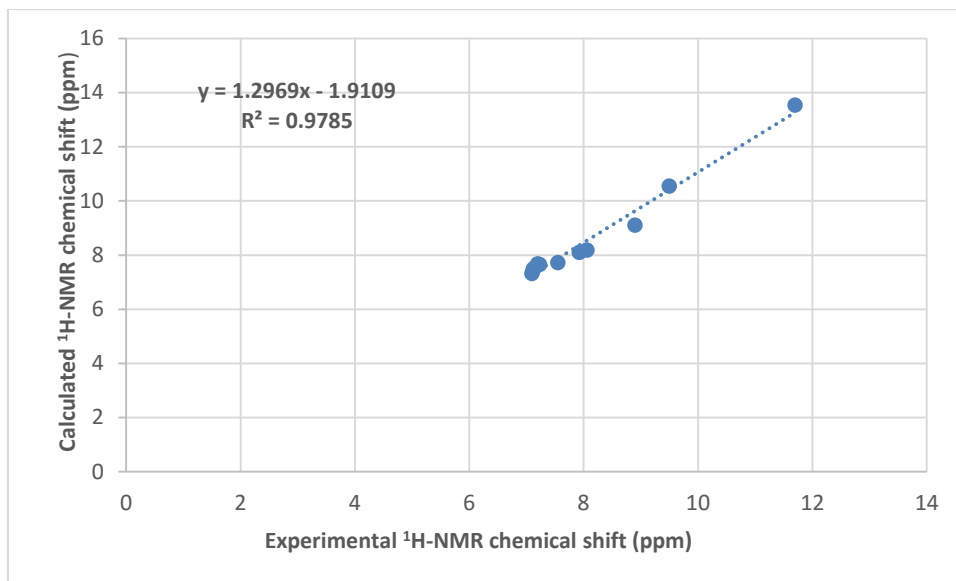


Figure 10: Correlation graph between experimental and calculated <sup>1</sup>H-NMR chemical shift.

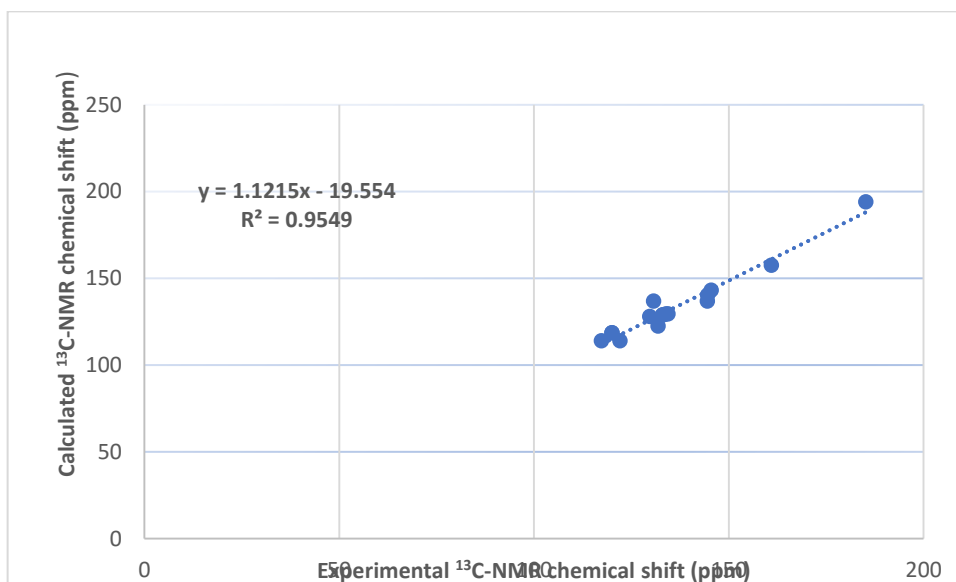


Figure 11: Correlation graph between experimental and calculated <sup>13</sup>C-NMR chemical shift.

In practice, NMR experiments do not measure the shielding directly, instead the common practice is to measure the chemical shifts as the change of resonance frequency of a nucleus relative to a given standard. Moreover, for historic reasons it is normally to reverse the frequency scale, i.e. nuclei more shielded than the standard are considered to have positive chemical shifts and those less shielded negative ones. The formal relation between the chemical shift and shielding tensors is given by:  $\delta = 1\sigma_{\text{iso}} - \sigma$ , where  $\delta$  is the chemical shift tensor,  $\sigma$  is the shielding tensor,  $1$  is the unit matrix and  $\sigma_{\text{iso}}$  is the isotropic value or trace of the shielding tensor of the standard reference used in the NMR experiments. Magnetic shielding tensors are given in units of ppm, and the J-coupling tensors are given in reduced SI units. This choice of units has been made so quantities given are independent of the isotope of the nucleus. The calculation of nuclear magnetic anisotropy shielding tensors via

gauge-including atomic orbital for nuclei C-1, H-31, C-32, H-34, is shown in **Figure 12**.

```

Calculating GIAO nuclear magnetic shielding tensors.
SCF GIAO Magnetic shielding tensor (ppm):
 1 C Isotropic = 37.9219 Anisotropy = 130.4967
    XX= 38.4213 YX= -2.6169 ZX= -0.0103
    XY= -16.6841 YY= -49.5753 ZY= 0.0137
    XZ= 0.0027 YZ= 0.0535 ZZ= 124.9197
31 H Isotropic = 18.3542 Anisotropy = 13.9898
    XX= 27.6348 YX= 1.7597 ZX= -0.0011
    XY= -2.8688 YY= 20.9899 ZY= -0.0022
    XZ= 0.0053 YZ= -0.0046 ZZ= 6.4378
Eigenvalues: 6.4378 20.9440 27.6807
32 C Isotropic = -2.7758 Anisotropy = 152.0748
    XX= -55.3609 YX= 34.3968 ZX= -0.0618
    XY= 31.2183 YY= -51.5738 ZY= 0.0191
    XZ= -0.0705 YZ= 0.0139 ZZ= 98.6074
Eigenvalues: -86.3295 -20.6052 98.6075
33 O Isotropic = -319.5260 Anisotropy = 1115.4079
    XX= -575.9141 YX= -236.2697 ZX= -0.3835
    XY= -318.2473 YY= -806.7431 ZY= -0.0567
    XZ= -0.4384 YZ= -0.1008 ZZ= 424.0791
Eigenvalues: -991.6498 -391.0076 424.0793
34 H Isotropic = 21.3425 Anisotropy = 3.3285
    XX= 22.6084 YX= -1.7560 ZX= 0.0005
    XY= 1.9942 YY= 23.5466 ZY= 0.0001
    XZ= -0.0001 YZ= -0.0023 ZZ= 17.8726
Eigenvalues: 17.8726 22.5935 23.5615
End of Minotr Frequency-dependent properties file 721 does not
exist.
End of Minotr Frequency-dependent properties file 722 does not
exist.
    
```

**Figure 12:** Screen shot of the out put wordPad file with the anisotropy shielding tensor

From the check point file of the GIAO calculations, shielding density maps are computed at shielding tensor (XX), diffuse functions of H-31, C-32, H-34, which may be related to the fact that polar systems with lone pairs in general require diffuse functions for a competent description, is well suited for the conception and interpretation of the H-31 of the hydrazone moiety and C-32& H-34 of the aldehyde group (**Figures 13, 14** and **15**). Maps showing streamlines and modulus of the current density yield valuable tools for interpreting the large out-of plane component of the magnetic susceptibility and the proton deshielding. [15, 44, 45]. The electron density yield valuable tools for interpreting component of the magnetic susceptibility and the proton, carbon deshielding. This is in good agreement with the ESP map of the molecule (**Figure 4**) which describes the active sites at the hydrazine moiety and the aldehyde group.

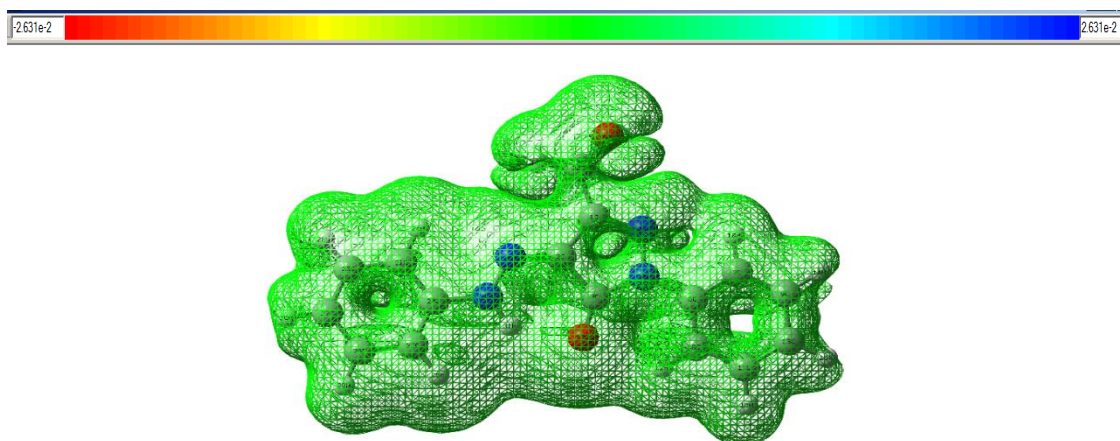


**Figure 13:** Shielding density as seen by nucleus H-31 in the XX direction mapped between the values of -2.632 to 2.632 on the current density isosurface at a value of 0.0004

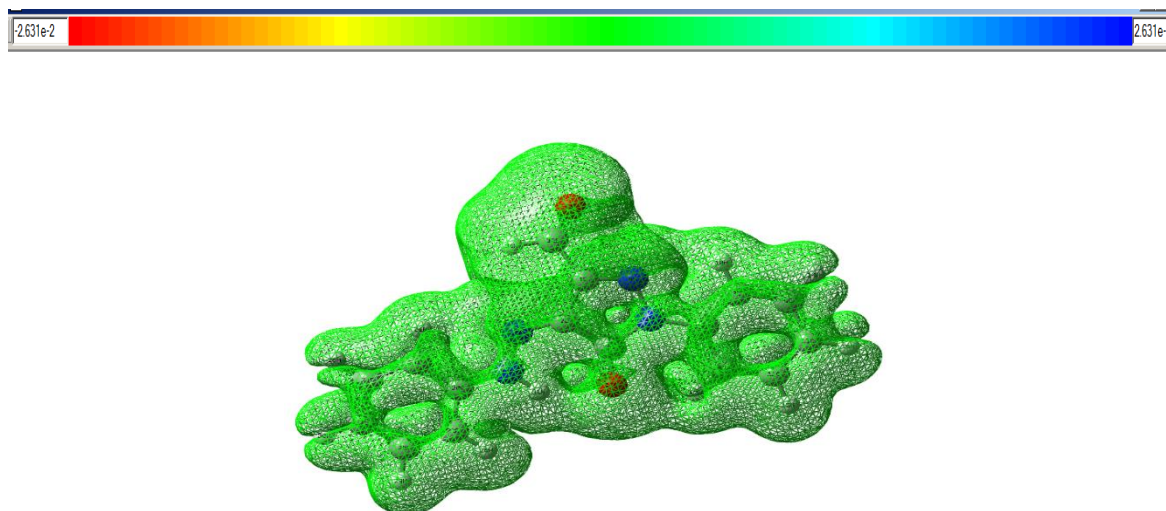


**Figure 14:** Shielding density as seen by nucleus C-32 in the XX direction mapped between the values of -2.631 to 2.631 on the current density isosurface at a value of 0.0004.

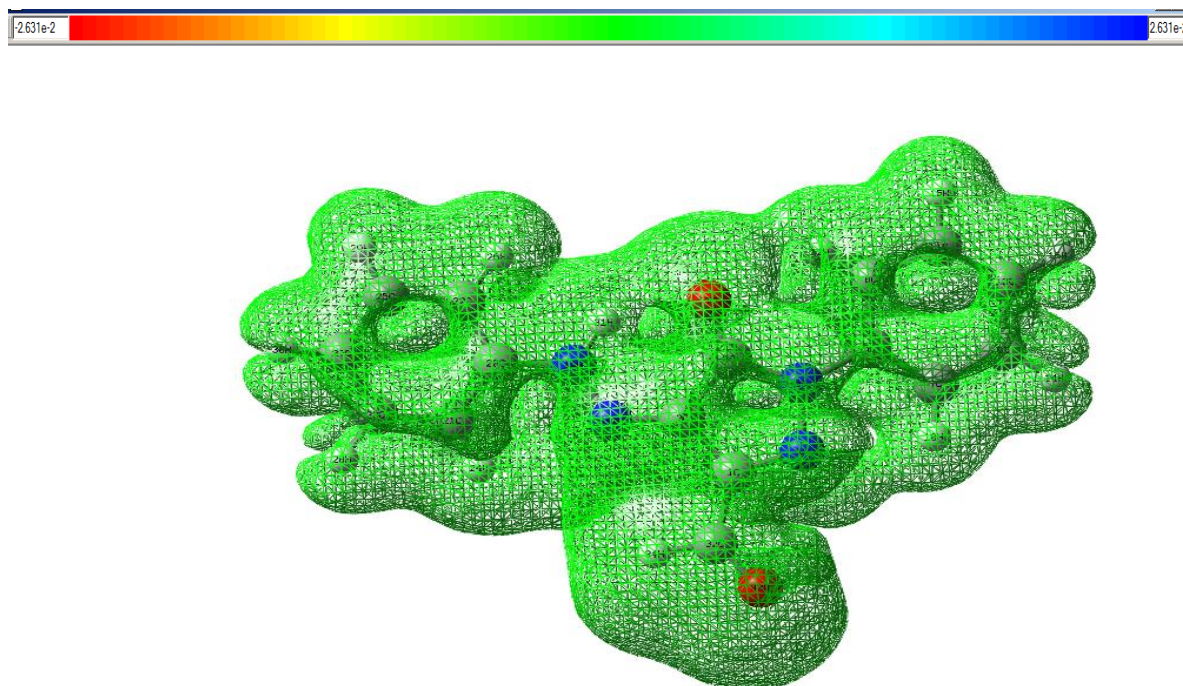


**Figure 15:** Shielding density as seen by nucleus H-34 in the XX direction mapped between the values of -2.631 to 2.631 on the current density isosurface at a value of 0.0004.

#### 4. Conclusion

In the present work, The B3LYP/ 6-311G (d, p) model within the DFT is used to optimize the structure of 5-oxo-1-phenyl-4-(2-phenylhydrazono)-4,5-dihydro-1H-pyrazol-3-yl)-1H-pyrazole-3-carbaldehyde and predict the

structure-properties relationships. Reactivity parameters calculated from the frontier orbitals help in prediction of chemical potential, hardness, softness, electrophilicity as well as nucleophilicity of the pyrazol-carbaldehyde molecule. Moreover, thermodynamic parameters verify the conclusions drawn from the molecular polarity. Computed and visualized MESP map surfaces enable exploration of molecular reactive sites (hydrazone moiety and the aldehyde group), which confirmed by mapping of shielding density by nuclei H-31, C-31, H-34 in the XX direction mapped on the current density.

## References

- [1]. W.J. Hehre, L. Radom, P. v. R. Schleyer, J. A. Pople. Ab Initio Molecular Orbital Theory. New York, NY, USA: John Wiley, 1986. <https://doi.org/10.1002/jcc.540070314>
- [2]. P. Hohenberg, W. Kohn. "In homogeneous electron gas". Phys. Rev., 136, B864–B871,1964 <https://doi.org/10.1103/PhysRev>
- [3]. R. G. Parr, W. Yang. Density Functional Theory of Atoms and Molecules. Oxford, New York. 1989.
- [4]. A. Szabo, N.S. Ostlund. Modern Quantum Chemistry. McGraw-Hill, New York. 1989.
- [5]. Dreizler R. M., E.K.U.Gross. Density Functional Theory. New York: Springer, 1990 .
- [6]. J.B. Foresman, A. Frisch. Exploring Chemistry with Electronic Structure Methods. Gaussian, Pittsburgh, PA. 1996.
- [7]. M. Springborg. Density Functional Methods in Chemistry and Materials Science. New York: Wiley, 1997
- [8]. I. Fleming. Frontier Orbitals and Organic Chemical Reactions. New York, NY, USA: John Wiley and Sons, 1976.
- [9]. P. Geerlings, F. de Proft, W. Langenaeker. "Conceptual density functional theory". Chemical Reviews. vol. 103(5),pp.1793–1873, 2003. <https://doi.org/10.1021/cr990029p>
- [10]. M. Cossi, N. Rega, G. Scalmani, V. Barone. "Energies, structures, and electronic properties of molecules in solution with the C-PCM solvation model". Journal of Computational Chemistry, 24(6), 669–681, 2003. <https://doi.org/10.1002/jcc.10189>
- [11]. L.R. Domingo, E. Chamorro, P. Pérez . "Understanding the reactivity of captodative ethylenes in polar cycloaddition reactions. A theoretical study". Journal of Organic Chemistry, 73, 4615–4624, 2008. <https://doi.org/10.1021/jo800572a>
- [12]. F. Zielinski, V. Tognetti, L. Joubert. "Condensed descriptors for reactivity: a methodological study". Chemical Physics Letters., 527, 67–72, 2012.
- [13]. L.R. Domingo. "A new C–C bond formation model based on the quantum chemical topology of electron density". RSC Advances., 4(61), 32415–32428, 2014.
- [14]. L.R. Domingo, M. Ríos-Gutiérrez, P. Pérez. "Applications of the conceptual density functional theory indices to organic chemistry reactivity". Molecules, 21(6),748-769, 2016.
- [15]. L.R. Domingo. "Molecular electron density theory: a modern view of reactivity in organic chemistry". Molecules, 21(10),1319-1333, 2016.
- [16]. Thom H. Dunning Jr. "Gaussian Basis Functions for Use in Molecular Calculations. I. Contraction of (9s5p) Atomic Basis Sets for the First- Row Atoms". J Chem Phys., 53, 2823,

1970. <https://doi.org/10.1063/1.1674408>
- [17]. B. Liu, A.D. Mclean. "Accurate calculation of the attractive interaction of two ground state helium atoms". *J Chem Phys.*, 59, 4557, 1973. <https://doi.org/10.1063/1.1680654>
- [18]. M.A. Thompson. Argus Lab 4.0.1. Planaria Software LLC, Seattle, WA. 2007.
- [19]. R. Poirier, R. Kari, I.G. Csizmadia. *Handbook of Gaussian Basis Sets*. New York: Elsevier, 2007.
- [110]. M.A. El Sekily, M.E. Elba, F. S. Foad. "Studies on Dehydro-L-Ascorbic Acid and Dehydro-D-Isoascorbic Acid Hydrazones". *Journal of Chemical Research*, 4, 296-297, 1999.
- [111]. M.A. El Sekily, M.E. Elba, F. S. Foad. "Some Heterocycles from Dehydro-L-Ascorbic Acid and Dehydro-D-Isoascorbic Acid". *Journal of the Indian Chemical Society*, 77, 168-171, 2000.
- [112]. M.A. El Sekily, S.H. Mancy, N.M.M. Hamada. "Synthesis, Characterization, and Antimicrobial activity of pyrazol-3-yl-pyrimidine, Pyrazole and Pyran derivatives". *Inter. J. Current. Research*, 11, (07), 5563-5570, 2019. DOI: <https://doi.org/10.24941/ijcr.36015.07.2019>
- [113]. R.G. Parr, R.A. Donnelly, M. Levy, W.E. Palke. "Electronegativity: The density functional view point". *J. Chem. Phys.*, 68, 3801-3807, 1978.
- [114]. E.J. Lien, Z.R. Guo, R.L. Li, C.T. Su. "Use of dipole moment as a parameter in drug receptor interaction and quantitative structure-activity relationship studies". *J. Pharm. Sci.*, 71, 641-655, 1982.
- [115]. R.G. Parr, R.G. Pearson. "Absolute hardness: companion parameter to absolute electronegativity". *J. Am. Chem. Soc.*, 105, 7512-7516, 1983.
- [116]. R.G. Parr, P.K. Chattaraj. "Principle of maximum hardness". *J. Am. Chem. Soc.*, 113, 1854-1855, 1991.
- [117]. W.P. Ozimin'ski, J.C. Dobrowolski, A.P. Mazurek. "DFT studies on tautomerism of C5-substituted 1,2,3-triazoles". *J. Mol. Struct.*, 651-653, 697-704, 2003.
- [118]. R.G. Parr, W. Yang. "Density Functional Theory of Atoms and Molecules". International series of monographs on chemistry, Oxford University Press, New York, 16, 1989.
- [119]. S. Zaater, A. Bouchoucha, S. Djebbar, M. Brahim. "Structure, vibrational analysis, electronic properties and chemical reactivity of two benzoxazole derivatives: Functional density theory study". *Journal of Molecular Structure*, 1123, 344-354, 2016.
- [30]. A.D. Becke. "Density functional thermochemistry. The rôle of exact exchange". *J.Chem.Phys.*, 98, 5648-5652. 1993. <https://doi.org/10.1063/1.464913>
- [31]. C. Lee, W. Yang, R.G. Parr. "Development of the Colle-Salvetti correlation-energy formula into a functional of the electron density". *Phys. Rev. B.*, 37, 785-789, 1988. <https://doi.org/10.1103/PhysRevB.37.785>
- [32]. R.I. Dennington, T. Keith, J. Millam, K. Eppinnett, W. Hovell, Gauss View Version, 2003.
- [33]. R. I. Dennington, T. Keith, J. Millam, Gauss View, Version 5. Semichem Inc., Shawnee Mission, 2009
- [34]. J. Cioslowski, D.J. Fox, Gaussian 09, Revision D.01; Gaussian Inc.: Wallingford, CT, USA, 2009.

- [35]. O. Tamer, B.S. Arslan, D. Avcı, M. Nebioglu, Y. Atalay, B. Cosut. "Synthesis, molecular structure, spectral analysis, and nonlinear optical studies on 4-(4-bromophenyl)-1-tert-butyl-3-methyl-1H-pyrazol-5-amine: a combined experimental and DFT approach". *J. Mol. Struct.*, 1106, 89-97, 2016.
- [36]. N.M.M. Hamada. "Synthesis, Spectroscopic Characterization, and Time Dependent DFT Calculations of 1-Methyl-5-phenyl-5H-pyrido[1,2-a] quinazoline-3,6-dione and Its Starting Precursor in Different Solvents". *Chemistry Open*, 7, 814–823. 2018. DOI: [10.1002/open.201800146](https://doi.org/10.1002/open.201800146)
- [37]. P. Jaramillo et al. "A further exploration of a nucleophilicity index based on the gas-phase ionization potentials". *J. Mol. Struct.: THEOCHEM*, 865(1-3), 68-72, 2008.
- [38]. S. Deuri, P. Phukan. "A DFT study on nucleophilicity and site selectivity of nitrogen nucleophiles". *Computational and Theoretical Chemistry*, 980, 49-55, 2012.
- [39]. R.K. Roy, S. Krishnamurti, P. Geerlings, S. Pal. "Local Softness and Hardness Based Reactivity Descriptors for Predicting Intra- and Intermolecular Reactivity Sequences: Carbonyl Compounds". *J. Phys. Chem. A.*, 102, 3746–3755, 1998.
- [40]. P.K. Chattaraj, B. Maiti. "Reactivity dynamics in atom-field interactions: A quantum fluid density functional study". *J. Phys. Chem. A.*, 105, 169–183, 2001.
- [41]. N. Prabavathi, S.N. Nayaki. "The spectroscopic (FT-IR, FT-Raman and NMR), first order hyperpolarizability and HOMO–LUMO analysis of 2-mercapto-4(3H)-quinazolinone". *Spectrochimica Acta Part A: Molecular and Biomolecular Spectroscopy*, 129, 572–583, 2014. <https://doi.org/10.1016/j.saa.2014.04.041>
- [42]. M.V.S. Prasad, K. Chaitanya, S.N. Udaya, V. Veeraiah. "Experimental and theoretical (HOMO, LUMO, NBO analysis and NLO properties) study of 7-hydroxy-4-phenylcoumarin and 5,7-dihydroxy-4-phenylcoumarin". *J. Mol. Struct.*, 1047, 216–228, 2013. <https://doi.org/10.1016/j.molstruc.2013.04.066>
- [43]. S. Fatma, A. Bishnoi, A.K. Verma. "Synthesis, spectral analysis (FT-IR, <sup>1</sup>H NMR, <sup>13</sup>C NMR and UV–visible) and quantum chemical studies on molecular geometry, NBO, NLO, chemical reactivity and thermodynamic properties of novel 2-amino-4-(4-(dimethylamino)phenyl)-5-oxo-6-phenyl-5,6-dihydro-4H-pyrano[3,2-c]quinoline-3-carbonitrile". *J. Mol. Struct.*, 1095, 112–124, 2015. <https://doi.org/10.1016/j.molstruc.2015.04.026>
- [44]. R.H. Mitchell. "Measuring Aromaticity by NMR". *Chem. Rev.*, 101(5),1301-1315, 2001. <https://doi.org/10.1021/cr990359>
- [45]. E. Steiner, P.W. Fowler, L.W. Jenneskens. "Counter- Rotating Ring Currents in Coronene and Corannulene". *Angew.Chem.*, 40, 362-366, 2001. [https://doi.org/10.1002/1521-3773\(20010119\)](https://doi.org/10.1002/1521-3773(20010119)).